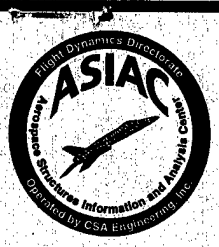

Aerospace Structures Information and Analysis Center

Design of a Variable Stiffness Spar

Report No. TR-97-01

January 1997

Approved for Public Release; Distribution is Unlimited

Operated for the Flight Dynamics Directorate by CSA Engineering, Inc.

REPORT DOCUMENTATION PAGE

Form Approved
OMB No. 0704-0188

1. AGENCY USE ONLY (Leave blank)	2. REPORT DATE	3. REPORT TYPE AND DATES COVERED
	January 1997	Final Report 09/22/95--10/25/96

4. TITLE AND SUBTITLE

Design of a Variable Stiffness Spar

5. FUNDING NUMBERS

C F33615-94-C-3200
PE 62201
PR 2401
TA 02
WU 99

6. AUTHOR(S)

Sridhar Kota, Joel Hetrick, and Laxman Saggere

7. PERFORMING ORGANIZATION NAME(S) AND ADDRESS(ES)

CSA Engineering, Inc.
2850 W. Bayshore Road
Palo Alto CA 94303-3843

8. PERFORMING ORGANIZATION REPORT NUMBER

ASIAC-TR-97-01

9. SPONSORING/MONITORING AGENCY NAME(S) AND ADDRESS(ES)

Flight Dynamics Directorate
Wright Laboratory
Air Force Materiel Command
Wright-Patterson AFB OH 45433-7542

10. SPONSORING/MONITORING AGENCY REPORT NUMBER

11. SUPPLEMENTARY NOTES

Approved for Public Release: Distribution Unlimited

12a. DISTRIBUTION/AVAILABILITY STATEMENT

12b. DISTRIBUTION CODE

13. ABSTRACT *(Maximum 200 words)*

Several studies have indicated that the performance of an aircraft can be considerably improved by adaptively varying the geometry of the wing to optimally suit the various flight conditions. The objective of this study was to seek a design concept for adaptively varying the torsional stiffness of an aircraft wing structure. Contemporary aircraft wing design consists of heavy cantilever beams (spars) which take the span-wise bending and shear loads. Metal ribs are spaced along the span in a chord-wise direction to maintain the airfoil shape. Metal skins are attached to this framework to stabilize the structure in torsion and provide stiffness. Recent studies showed that performance of an aircraft could be considerably improved by adaptively varying the torsional load carrying capacity of the wing spar. Hence, design concepts for adaptively varying the torsional stiffness of an aircraft wing spar were studied.

Three different concepts were considered:

1. Variable torsional constant by varying the member cross-section.
2. Variable axial shear stress by activating/inactivating some member elements.
3. Preventing one of more cross-sections along the length of the member from warping.

The first two concepts are discussed in this report. A comparison of the effectiveness of these two concepts through a finite element analysis are also presented.

14. SUBJECT TERMS

Variable Stiffness, Smart Structures, Adaptive Wings, Torsional Stiffness, Finite Element Analysis

15. NUMBER OF PAGES

35

16. PRICE CODE

17. SECURITY CLASSIFICATION OF REPORT	18. SECURITY CLASSIFICATION OF THIS PAGE	19. SECURITY CLASSIFICATION OF ABSTRACT	20. LIMITATION OF ABSTRACT
Unclassified	Unclassified	Unclassified	SAR

FOREWORD

This report was prepared by the Aerospace Structures Information and Analysis Center (ASIAC), which is operated by CSA Engineering, Inc. under contract number F33615-94-C-3200 for the Flight Dynamics Directorate, Wright-Patterson Air Force Base, Ohio. The report presents the work performed under ASIAC Tasks No. T-19 and T-20. The work was sponsored by the Vibration and Aeroelasticity Branch, Structures Division, Flight Dynamics Directorate, WPAFB, Ohio. The technical monitors for the task were Major Kimberly Demoret of the Acoustic and Sonic Fatigue Branch, and Lt. Damin Siler of the Vibration and Aeroelasticity Branch. The study was performed by Dr. Sridhar Kota of the University of Michigan, with the assistance of graduate research associates, Joel Hetrick and Laxman Saggere, under contract to CSA Engineering Inc.

This technical report covers work accomplished from September 1995 through October 1996.

TABLE OF CONTENTS

SECTION		PAGE
1	Introduction	1
2(a)	Variable cross-section concept	1
2(b)	Variable axial shear stiffness concept	4
3	Comparison of the two concepts by finite element analysis	8
4	Development of the Variable Cross-section Concept	11
5	Analysis	12
6	Implementation of the variable cross section concpet	17
7	Conclusions and Recommendations	19

LIST OF FIGURES

FIGURE		PAGE
1	Design concept for varying torsional stiffness by varying the cross-section of the spar. Movable webs: (a) The initial "stiff" state. (b) The final "relaxed" state.	5
2	Design concept for varying torsional stiffness by varying the cross-section of the spar. Activate-Deactivate type webs: (a) initial "stiff" state. (b) Final "relaxed" state.	5-6
3	Design concept for varying torsional stiffness by varying the axial shear stiffness of the spar. (a): The initial "stiff" state. (b): The final "relaxed" state.	7
2*	Finite element analysis of the variable cross-section concept.	9
3*	Finite element analysis of the variable axial shear stiffness concept.	10
4	Comparison of torsional stiffness based on the size of sectorial area enclosed.	12
5	Illustration of two possible schemes to vary the sectorial area.	13
6	A three cell box beam section.	14
7	A single cell box beam section.	15
8	A 3-D Plot of the ratio β/β^* as a function of a and x.	16
9	Practical implementation of the variable cross section collapsible-cell design concept.	18
10	Physical embodiment of a collapsible web idea.	20
11(a)	Sketch of Wright Lab Wing box test bed.	21
11(b)	Cross-section of a variable stiffness spar based on the dimensions specified in Figure 11(a).	22
12	Variable Stiffness Spar constructed at the University of Michigan using the variable cross-section concept.	23

LIST OF FIGURES

FIGURE		PAGE
13	Variable Stiffness Spar constructed at the University of Michigan - Spar shown in locked and unlocked positions.	24
14	Variable Stiffness Spar constructed at the University of Michigan. test apparatus.	25
15	Applied torque versus the angle of twist of the variable stiffness spar when spars are locked. The hysteresis effect suggests slippage between the wen and the flange. (a) Left end spar. (b) Right end spar	26
16	Applied torque versus the angle of twist of the variable spar when spars are unlocked. (a) Left end spar. (b) Right end spar.	27
17	Various measurements made on the modified variable stiffness spar. Deflections are measured at 30 inches from the center pivot. The results showed a 30% reduction in torsional stiffness of the spar when the end spars are unlocked.	28
18	Recommendation to use interlocking teeth between the flange and the web in the end spars to prevent slippage in the locked state.	29

LIST OF TABLES

TABLE		PAGE
1	Comparison of the variable cross-section and variable axial shear concepts	11

Design of a Variable Stiffness Spar

Principal Investigator: Sridhar Kota, Associate Professor

1. Introduction

Several studies have indicated that the performance of an aircraft could be considerably improved by adaptively varying the geometry of the wing to optimally suit the various flight conditions. The objective of this study is to seek a design concept for adaptively varying the torsional stiffness of an aircraft wing structure.

In a previous report, based on rudimentary data, we discussed some of the ways to adaptively vary the torsional stiffness of only a *spar* of the wing structure.

Contemporary aircraft wing design consists of heavy cantilever beams called spars which take the span-wise bending and shear loads. Metal ribs are spaced along the span in a chord-wise direction to maintain the airfoil shape. Metal skins are attached to this framework to stabilize the structure in torsion and provide stiffness.

Conventionally wing spars are of fixed geometry cross-section. It was recently studied that by adaptively varying the torsional load carrying capacity of the wing spar, the performance of an aircraft could be considerably improved. Hence, a design concept for adaptively varying the torsional stiffness of an aircraft wing spar is desired.

Three different concepts were considered:

1. Variable torsional constant by varying the member cross-section.
2. Variable axial shear stress by activating/inactivating some member elements.
3. Preventing one or more cross-sections along the length of the member from warping.

The first two concepts are discussed below. A comparison of the effectiveness of these two concepts through a finite element analysis is also presented below.

2 (a) Variable cross-section concept

In the case of a prismatic torsion member with constant cross-section, the torque applied on the member and the resulting twist are related by:

$$T = GJ\theta$$

where T = the torque applied, θ = the twist per unit length, J = the torsional constant for the cross-section, G = Shear modulus of the material of the member. The product GJ is called the torsional rigidity (stiffness) of the member. The torsional constant J, depends entirely on the shape of the

cross-section and can be expressed as a function of the principle dimensions of the cross-section. For a simple circular cross-section of radius r, the torsional constant turns out to be the polar moment of inertia of the cross-section, i.e., $J = \pi r^4/2$. For some non-circular cross-sections, the exact analytical solutions and the torsional constants can be found by either the theory of elasticity, or the Prandtl's stress function. For other torsion members whose cross-sections are too complex for exact analytical solutions, approximate solutions are obtained by Prandtl's elastic-membrane (soap-film) analogy.

An important class of torsion members are those with thin walls. Included in the class of thin-walled torsion members are open and box sections which are widely employed in the aircraft structures. Approximate solution for a box section obtained by the membrane analogy can be expressed by the following two relations:

$$T = 2A\tau t$$

$$\frac{1}{A}\oint \tau dl = 2G\theta$$

where A = the area enclosed by the mean perimeter of the box section

T = shear stress (assumed constant) through the thickness of the wall of the cross-section, and

dl = infinitesimal length of the perimeter of the box-section.

For a thin-walled tubular structure of wall thickness t and a cross-section of mean radius R, the above relations may be combined and expressed as

$$T \approx 2\pi R^3 tG\theta$$

Here we notice that for a box-section, $J \approx 2pR^3t$.

Thus, for a torsion member of either solid cross section or thin walled box section, and made of a given isotropic material, the torsional stiffness can be varied by altering the torsional constant, J. Since J depends on the shape of the cross-section, it seems a direct approach to vary the cross section of the torsion member to obtain a varied torsional stiffness.

The following general observations may be useful in <u>deriving a concept to vary the torsional stiffness</u>:

- Of the two sections having same the area, the one more nearly circular is stiffer. Of the sections shown below, the square section (B) is stiffer than the rectangular section (A), and the circular section (C) is stiffer than both rectangular and a square section of the same areas. This may be understood from the Prandtl's membrane analogy as square membrane in (B) enclosing greater volume and therefore carries greater torque than the of the rectangular membrane in (A) and the circular membrane in (C) enclosing greater volume than both the square and the rectangular membranes.

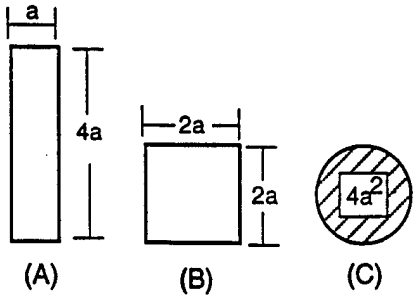

- Although any extension, whatever of the section, increases its torsional stiffness, narrow outstanding flanges and similar protrusions have little effect.

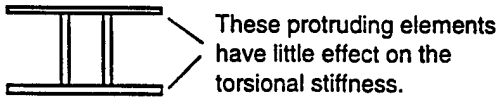

- Any member having a narrow section, such as a thin plate, has practically the same torsional stiffness when flat as when bent into the form of an open tube or into channel or angle section. The section (A) shown below has the same torsional stiffness when bent into the shape shown in (B). Again, this observation may be quickly understood from the Prandtl's membrane analogy.

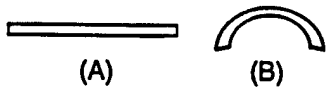

- For hollow sections, strength and stiffness depend largely upon the area enclosed by the median boundary. For example, although the sections (A) and (B) below are of same sectional area, the section shown in (B) below encloses larger median area than that of section (A) and hence it is stiffer than section (A). For this reason, circular tube is more stiffer and stronger than one of any other form.

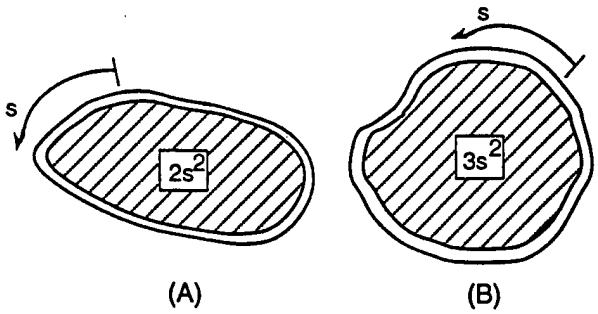

The last observation is particularly useful for our purpose since the spars in aircraft wings are mostly of box sections. Based on this idea of modifying the area enclosed by the median boundary of the thin walled box section, the design concepts shown in Figures 1 and 2 are proposed. In Fig. 1, the section is basically a I-section with two moving webs that slide inward and outward from the

central web. When the two outer webs are in drawn out extreme position (Figure 1a), the section walls enclose maximum area and hence the member provides the maximum torsional stiffness. And, when the webs are in the drawn-in position (Figure 1b), the section walls enclose minimum area, thereby providing a relaxed torsional stiffness. The moving webs may be split into several spanwise sections so that the torsional stiffness may be varied along the spanwise by positioning the moving webs at different distances from the central web along the span.

An interesting advantage of this design concept is that there will be absolutely no change in bending stiffness of the spar at all. This is because the moment of inertia of the spar about the chord-wise axis (which controls the bending stiffness of the spar for vertical loads) remains unchanged irrespective of the location of the moving webs along the chord axis.

If the sliding of webs inside a spar could be a problem due to operating loads, the active webs could be designed as in Figure 2. In this case, there are two webs of variable length on each side of the fixed central web. Variation in the length of a web can be achieved by a telescoping arrangement. When maximum torsional stiffness is desired the extreme outward webs may be activated (Figure 2a) and when minimum torsional stiffness is desired the interior webs may be activated (Figure 2b). Interior webs are not essential from the viewpoint of relaxed torsion, but they are required if it is desired to keep the bending stiffness unchanged in either configuration.

2 (b) Variable axial shear stiffness concept

The other design concept proposed by the WPAFB for variable torsional stiffness is to vary the axial shear stiffness of the spar. The proposed concept is shown in Figure 3. The figure shows two flanges connected by several cross-pieces inclined to the flange surfaces. Alternate cross-pieces are of bi-state connection type, i.e., they can be connected or disconnected from the flanges by either a hydraulic or electrical actuation. When a lower torsional stiffness of the spar is desired, the alternate cross-piece elements are disconnected from the flanges thereby eliminating them from the load path.

The torque applied at the end of a prismatic member is resisted by shear stress in the plane of end section of the member. The equations of equilibrium require the shear stress in the end plane in turn to be in equilibrium with an axial shear stress of equal magnitude. Thus, any weakening of axial shear stress would change the state of stress equilibrium which causes the end-plane shear stress to exceed the axial stress and thereby provides more yielding in torsion.

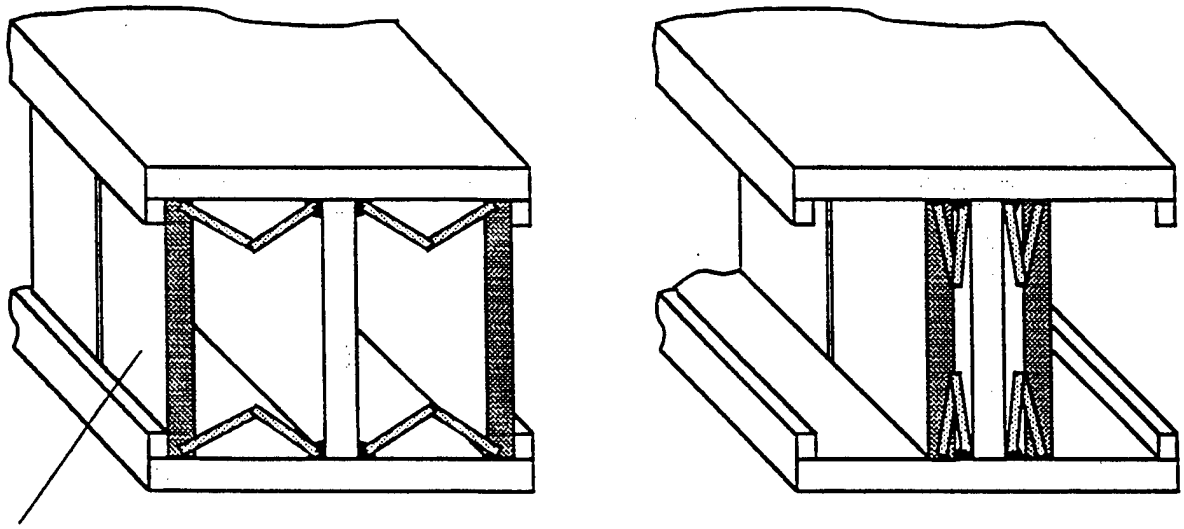

If necessary, the active webs may be split into several spanwise segments to obtain spanwise variation of torsional stiffness.

(a) (b)

Figure 1: Design concept for varying torsional stiffness by varying the cross-section of the spar. Movable webs: (a) The initial "stiff" state. (b) The final "relaxed" state.

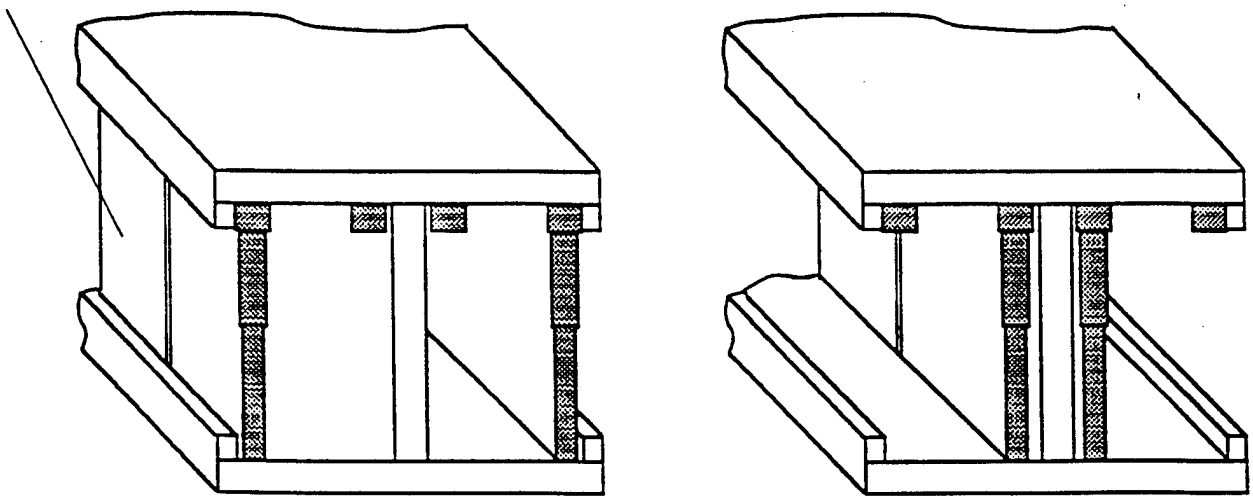

(c) (d)

Figure 2: Design concept for varying torsional stiffness by varying the cross-section of the spar. Activate-Deactivate type webs: (a) Initial "stiff" state. (b) Final "relaxed" state.

Figure 2 (continued): Two other concepts for variable stiffness spar that were generated during brainstorming sessions.

Small web segments changing orientations w.r.t the main web at the center

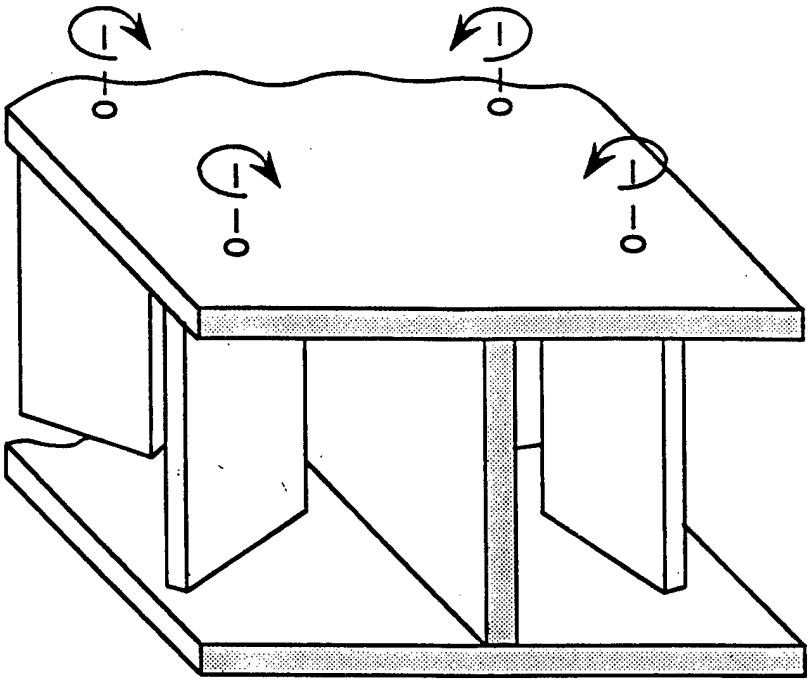

Folding Flanges

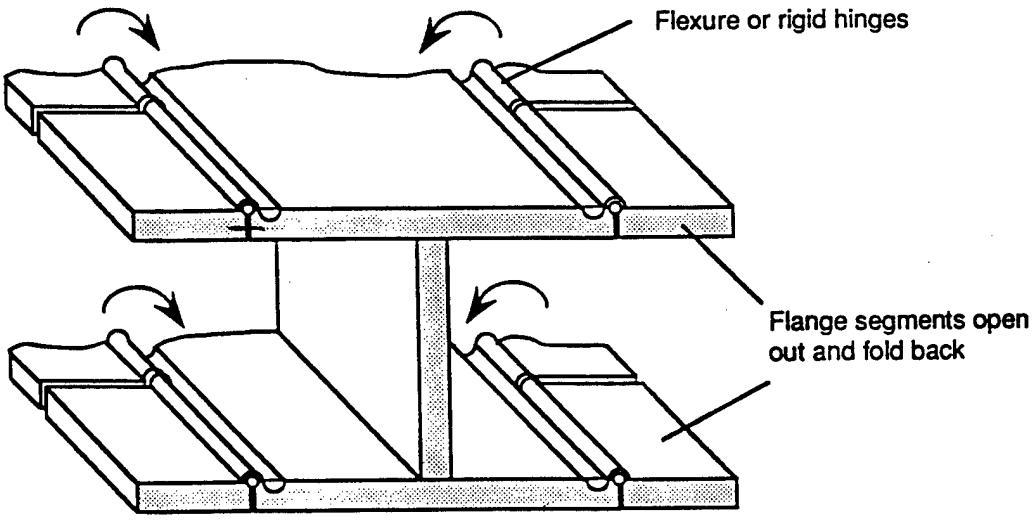

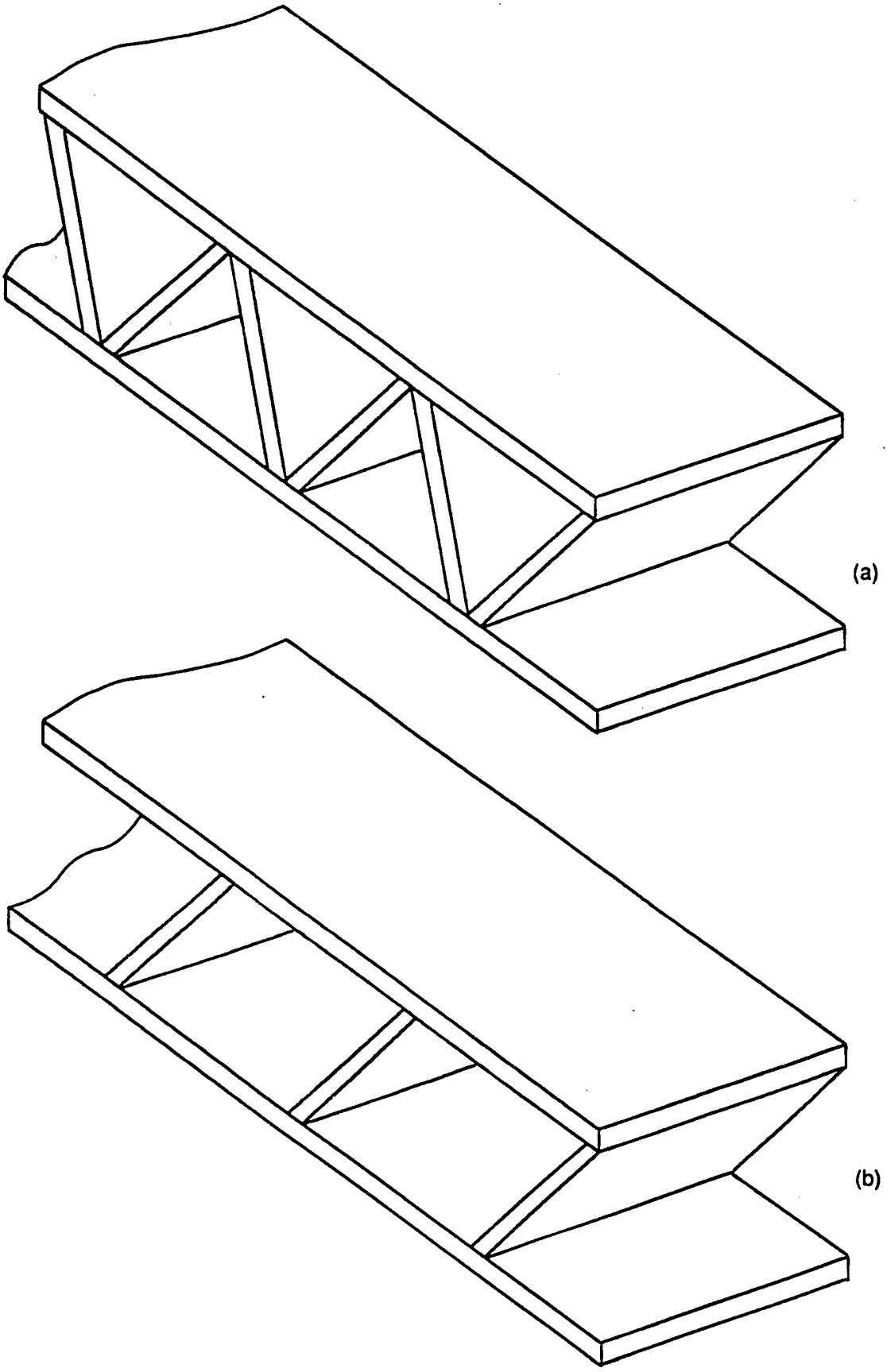

Figure 3: Design concept for varying torsional stiffness by varying the axial shear stiffness of the spar. (a): The initial "stiff" state. (b): The final "relaxed" state.

However, controlling purely the axial shear of a spar (or any structural member for that matter) seems to be practically not feasible. For instance, in the proposed design concept, the elimination of cross-pieces from the load path amounts to removal of material from the spar and hence, it not only reduces the axial shear stiffness of the spar, but also weakens its normal (axial compressive) strength and reduces its bending stiffness significantly. Thus, this approach has the disadvantage of influencing the load carrying capability of the spar in all directions while the interest is in reducing torsional stiffness alone.

3. Comparison of the two concepts by finite element analysis

A strict comparison of the effectiveness of the two proposed designs is not possible because a clear basis for such comparison has not been established yet. However, a rough comparison of their effectiveness can be made based on the amount of variation of torsional stiffness that each design provides under identical torque load and identical sizes of the spars. To make such a comparison, finite element analyses were performed on the two designs of spars of identical overall sizes. The length, width and height of the spars were assumed to be 4m, 0.25m, and 0.25m respectively. The cross-pieces were assumed to be inclined at 45° angle to the flange surfaces. All of the plates comprising the spars (i.e., flanges and webs) were assumed to be 2 cm thick.

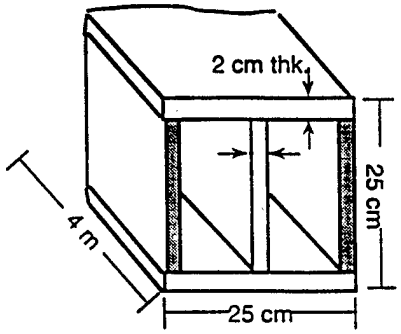

To enable identical application of torque loads on both the designs, an end plate was attached to the end of the spar in each case. The spars were modeled as cantilever structures in the finite element software ANSYS using shell elements. Each of the two designs was analyzed in two states: the initial "stiff" state and the final "relaxed" (or compliant) state under a torque load of 1000 N-m applied at the center of the end plate at the free end of the spars. Figures 2* and 3* show the finite elements analysis of the two concepts shown in Figure 2 and 3 respectively. The resulting twist, measured at the point of application of the torque, is proportional to the torsional stiffness of the spar in each case. The spars were also analyzed under a vertical force (perpendicular to the flange surfaces) of 10 KN applied at the tip of the cantilevers to compare the bending stiffness of the spars in the two design concepts. The tip deflection of the cantilever, in each case, is proportional to the bending stiffness of the spar. The results are shown in the following table:

Figure 2*: Finite element analysis of the variable cross-section concept.

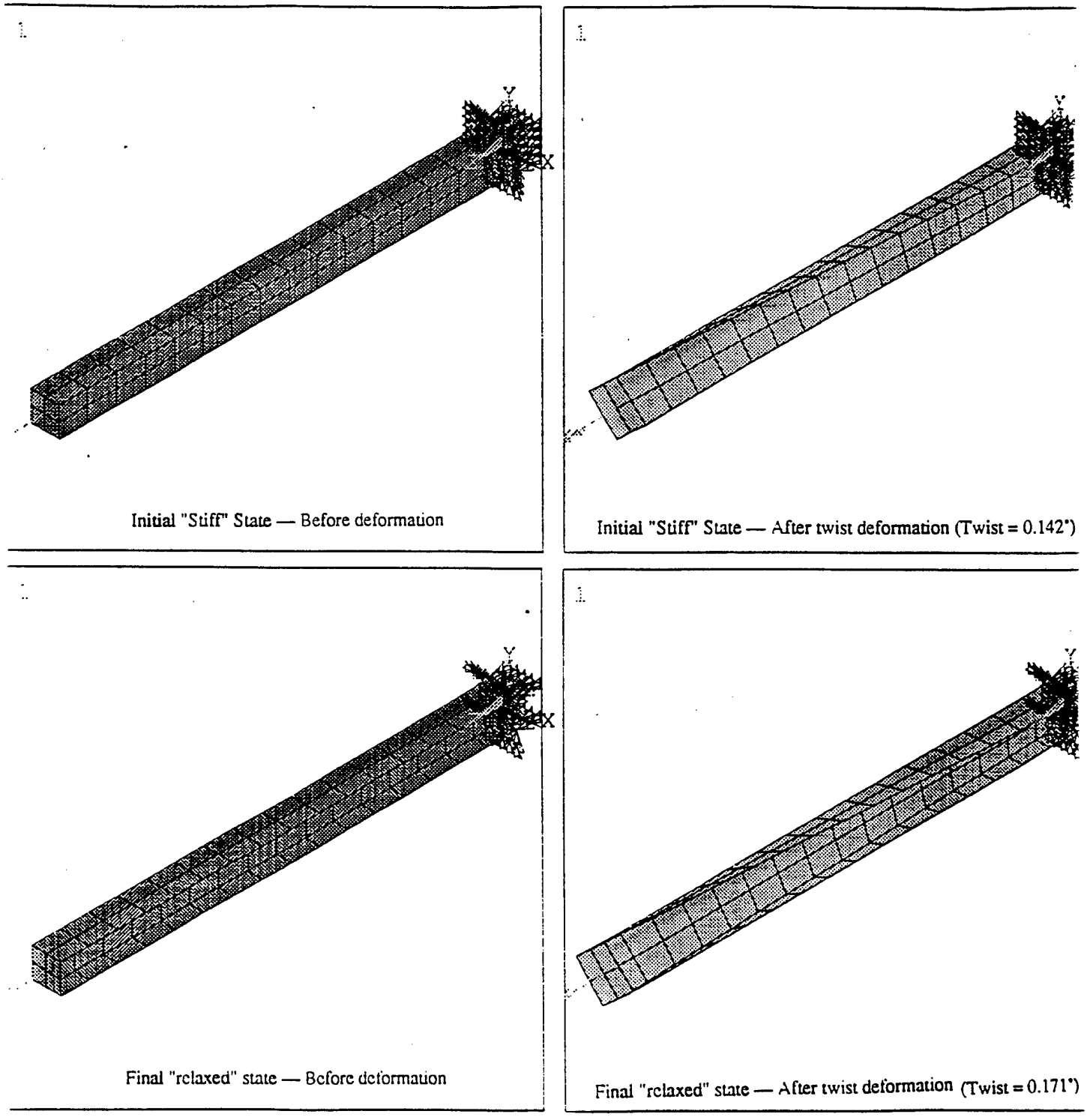

Figure 3*: Finite element analysis of the variable axial shear stiffness concept.

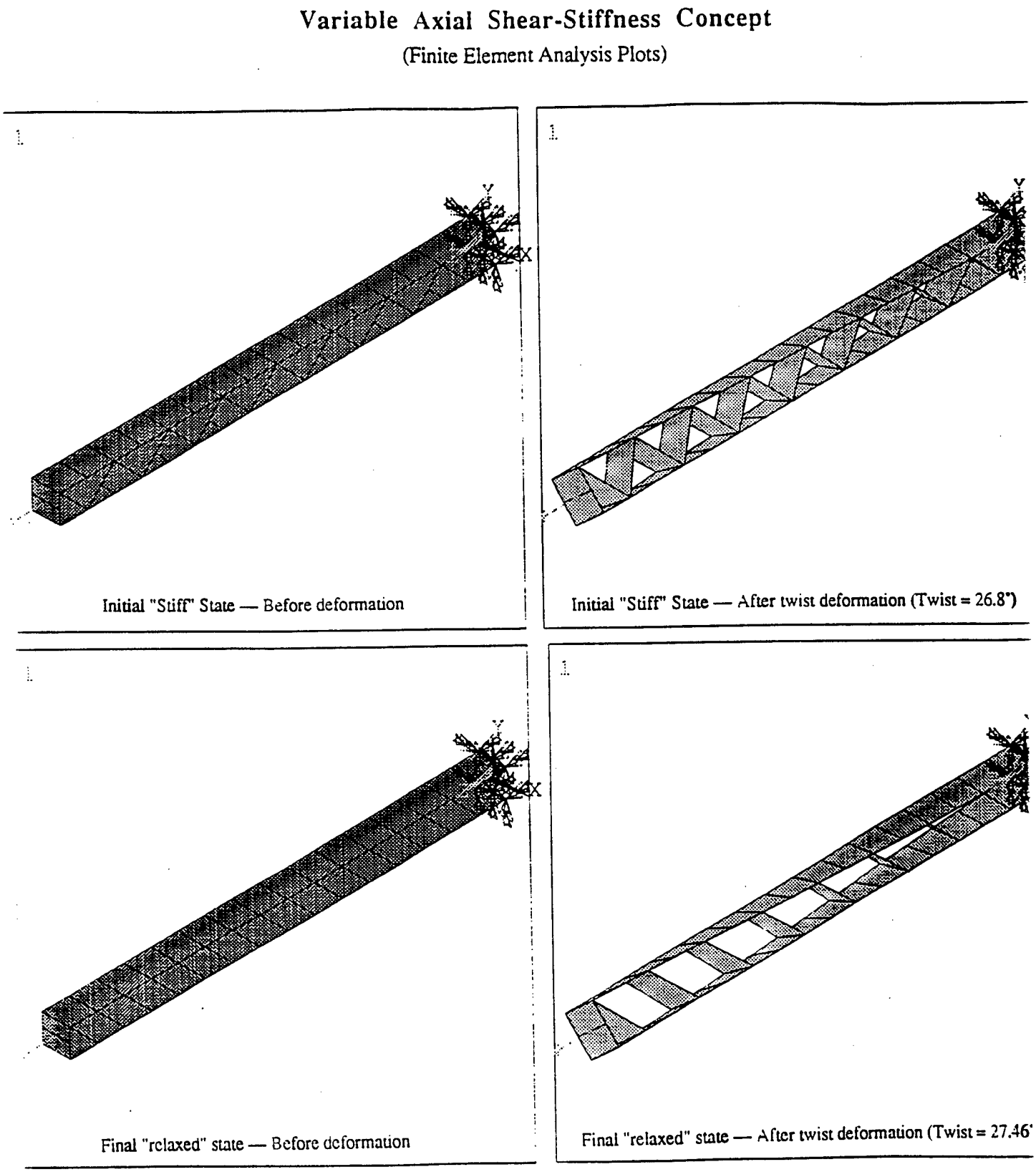

Design	The initial "stiff" state		The final "relaxed" state		Variation in stiffness	
	Twist	Tip deflection in bending	Twist	Tip deflection in bending	Torsional	Bending
Variable cross-section	0.142°	4.57 mm	0.171°	4.57 mm	20.5 %	None
Variable axial shear	26.80°	6.85 mm	27.46°	29.7 mm	2.46 %	4.3 times

Table 1: Comparison of the variable cross-section and variable axial shear concepts

4. Development of the Variable Cross-section Concept

Next, we concern ourselves with the task of obtaining a design concept to vary the torsional stiffness of the wing structure *as a whole*. The variable stiffness design sought has to be compatible with the rest of the design.

The torsion load acting on the wing (along the span) is resisted by built-up box structures. In many designs, the leading edge cell is often neglected in resisting torsional moments due to cutouts, etc. and thus the remaining cell(s) are assumed to provide the entire torsional resistance. For the purpose of a design concept, without any loss of generality, the cell structure resisting the torsional moment could be assumed to be rectangular cellular box such as the three celled beam shown in Figure 4. The question we have to address here is *how to vary the torsion stiffness of the cellular box structure with minimal changes to the structure?*

A general fact about the thin walled closed beams—discussed in other reports—is that its strength and stiffness depend largely upon the area enclosed by the median boundary or the sectorial area of the section. In general, the larger the sectorial area enclosed, the higher the torsional stiffness. For instance, in Figure 1 the torsional stiffness of the three celled beam with sectorial of area 3A is much greater than the torsional stiffness of the single celled beam with sectorial area A. Thus, a theoretical design concept for variable torsional stiffness would be to toggle the median area of the cell to be small in the *compliant* state, and larger in the *stiff* state.

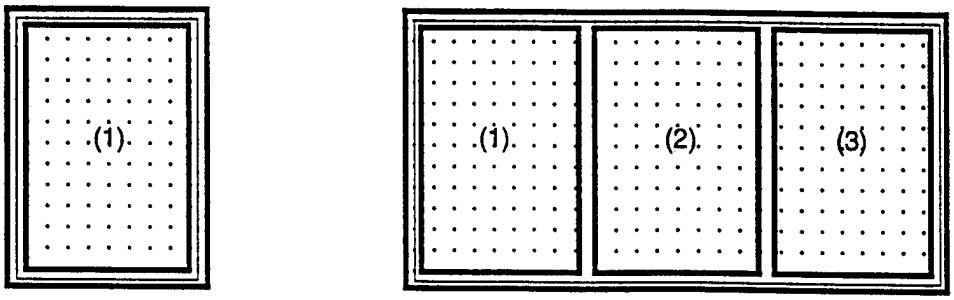

Sectorial area = A

Sectorial area = 3A

Figure 4: Comparison of torsional stiffness based on the size of sectorial area enclosed.

The above concept of varying the sectorial area can be implemented in the box beam of the wing structure in at least two ways, Scheme 1 and Scheme 2, as illustrated in Figure 5. In Scheme 1, the sectorial area of the box can be increased by "moving" the internal webs farther apart. Alternatively, the sectorial area increase can be achieved by adding webs to the beam there by making it a three celled section as shown in Scheme 2. Since physically moving the webs is not practicable in the aircraft wings, implementation of Scheme 1 requires activation/deactivation of the internal and external webs. That means, in Scheme 1, a change of the stiffness state of the wing from "compliant state" to "stiff state" (or vice-versa), requires the actuation of four webs—deactivation of the two internal webs and activation of the two external webs (or vice-versa). On the other hand, for the same change of state, Scheme 2 requires only two actuators—activation of the two outer webs (to convert a single celled section to a three celled section). Thus, from practical viewpoint of change in geometry required, Scheme 2 is more efficient than Scheme 1.

In the compliant state (in either Scheme) the extending flanges from the central cell remain attached to the central cell; however, the flange extensions contribute minimally, if any, to the torsional resistance and hence they can be neglected in the torsional resistance calculation for the single cell case in collapsed state. We are now left with the design question: *how does the torsional stiffness vary with the cell dimensions?* In order to answer this question, we carry out the following analysis.

5. Analysis

Notation:

T = Net torsional moment on the wing structure.

h = Height of the cell structure.

w = Width of the each of the two outer cells.

x = Ratio of the width of the central cell section to the width of an outer cell.

q = Shear flow in the cell walls.

G = Sectorial area of each cell.

b = Twist per unit length of the box section in the stiff state.

b^* = Twist per unit length of the box section in the relaxed state in Scheme 1.

b^{**} = Twist per unit length of the box section in the relaxed state in Scheme 2.

n= number of closed cells.

G= Shear modulus of the material of the box beam.

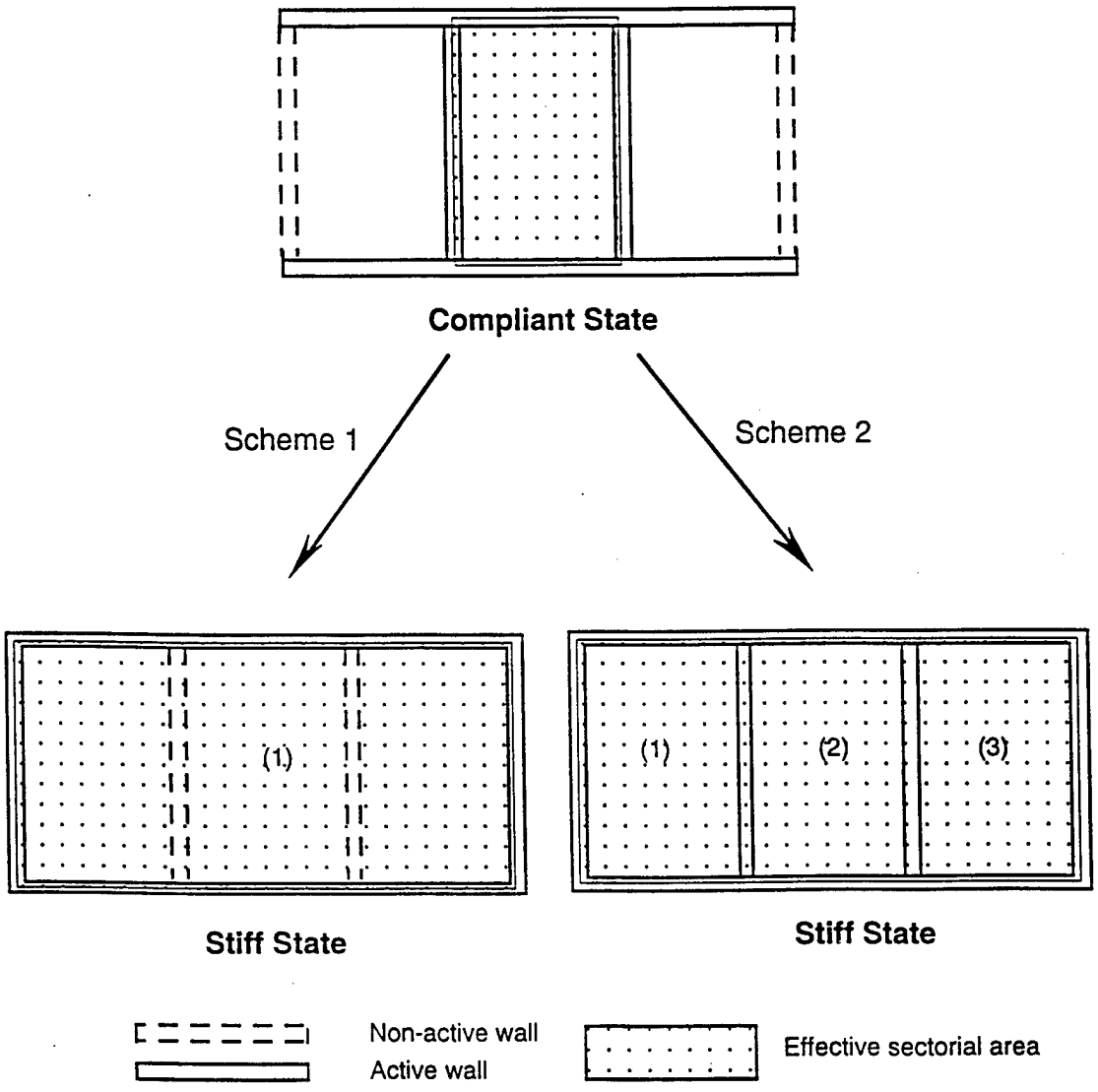

Fig. 5: Illustration of two possible schemes to vary the sectorial area.

From the discussion in the previous section, it is clear that our design interest would be to minimize the ratio b/b^*. Hence, in this analysis we seek the ratio b/b^* as a function of the cell dimensions in order to study the effectiveness of each of the cell dimensions on the ratio. First, we derive the expressions for b b^*, and b^{**} separately, and then obtain the ratio b/b^*.

Expression for b ("Stiff" state of the wing in Scheme 1):

In a multi-cell hollow sections, the rate of twist b, the geometry of the box beam, and the applied torque are related through the shear flow in the cell walls as given by the following equations:

$$\beta = \frac{1}{2G\Gamma_i}\left(\oint \frac{q}{t} ds\right)_i \quad \text{and} \quad T = 2\sum_{i=1}^{n} \Gamma_i q_i$$

Applying these equations to the three celled beam shown in Figure 6, we obtain,

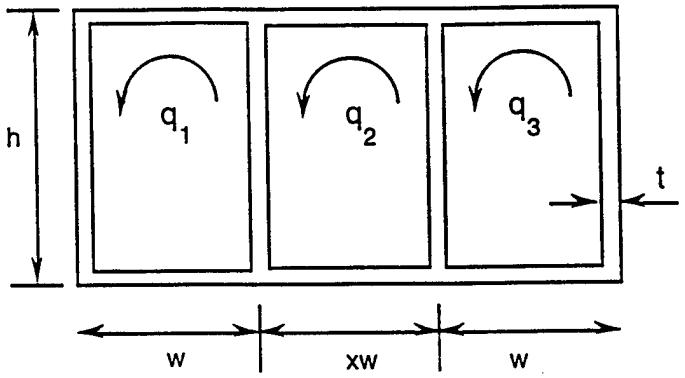

Figure 6: A three cell box beam section

$$2G\beta = \frac{1}{wh}\left[\frac{2w+h}{t} q_1 + \frac{h}{t}(q_1 - q_2)\right]$$

$$2G\beta = \frac{1}{xwh}\left[\frac{2xw}{t} q_2 + \frac{h}{t}(q_2 - q_1) + \frac{h}{t}(q_2 - q_3)\right]$$

$$2G\beta = \frac{1}{wh}\left[\frac{2w+h}{t} q_3 + \frac{h}{t}(q_3 - q_2)\right]$$

Solving for q_1, q_2, and q_3, we obtain,

$$\begin{bmatrix} q_1 \\ q_2 \\ q_3 \end{bmatrix} = \begin{bmatrix} \frac{2xw+xh+2h}{2(2xw^2+2hw+2xwh+h^2)} \\ \frac{h+xw+xh}{(2xw^2+2hw+2xwh+h^2)} \\ \frac{2xw+xh+2h}{2(2xw^2+2hw+2xwh+h^2)} \end{bmatrix} (2G\beta)(wht)$$

$$T = 2\sum_{i=1}^{3} \Gamma_i q_i$$

$$= \frac{4G\beta w^2h^2t(2xw+2xh+2h+x^2w+x^2h)}{(2xw^2+2hw+2xwh+h^2)}$$

Solving for b from the above equation, we get,

$$\beta = \frac{T(2xw^2+2hw+2xwh+h^2)}{4Gw^2h^2t(2xw+2xh+2h+x^2w+x^2h)}$$

This is the rate of twist of the three celled beam as a function of the cell dimensions and the applied torque.

Expression for b^* ("Relaxed" state of the wing):

The rate of twist in a single celled hollow section is obtained from the Bredt's formula:

$$\beta = \frac{q}{4G\Gamma^2}\oint\frac{ds}{t}$$

Applying this formula to the single celled box beam in compliant state, we obtain,

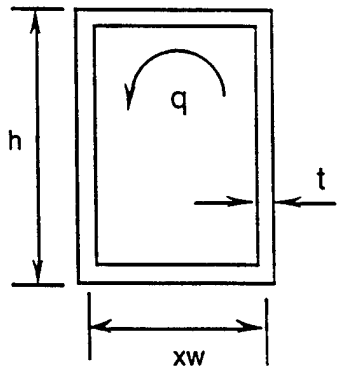

Figure 7: A single cell box beam section.

$$\beta^* = \frac{T(xw+h)2}{4Gh^2x^2w^2t}$$

This is the rate of the twist of the single celled box beam as a function of the cell dimensions and the applied torque.

Dividing the expression for b by the expression for b^* we have,

$$\frac{\beta}{\beta^*} = \frac{(4xw^3 + 2h^2w + 4hxw^2 + h^3)x^2}{4(2xw^2 + h^2 + xwh + x^2w^2 + x^2wh)(xl + h)}$$

$$= \frac{(4x + 2a + 4xa + a^3)x^2}{4(2x + a^2 + ax + x^2 + x^2a)(x + a)}$$

where $a = \frac{h}{w}$.

The ratio b/b^* represents the ratio of twist of the spar in its "stiff" state to the twist in its "relaxed" state under identical torque loads. In order to achieve maximum variation of the twist with minimum variation in the geometry of the member, we need to keep the ratio b/b^* as small as possible. The ratio b/b^* can be varied by controlling the two variables, a and x. To understand how the ratio b/b^* varies with respect to the two variables, a 3-D plot of the ratio b/b^* as a function of a and x is shown in Figure 8.

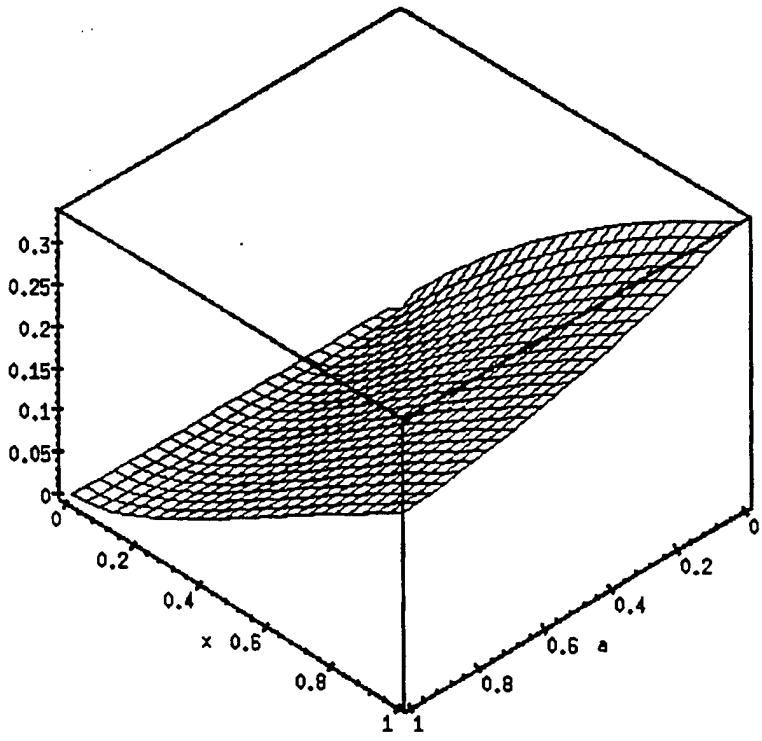

Figure 8: A 3-D Plot of the ratio $\frac{\beta}{\beta^*}$ as a function of a and x.

From the plot, we can observe that the ratio $\frac{\beta}{\beta^*}$ varies considerably with respect to both a and x. Since we are interested in minimizing the ratio $\frac{\beta}{\beta^*}$, a small ratio can be maintained by either designing x to be as small as possible or a to be as high as possible. However, due to typical aspect ratio of the aircraft wings, a cannot be made too high. Hence, alternatively, x could be designed to be very small. Typical variations of the twist in the "relaxed" state as a percentage of the twist in the "stiff" state is shown below.

a	x	$\frac{\beta}{\beta^*}$	Percentage variation in twist of the wing
0.1	1	0.3129°	68%
0.5	0.5	0.119	88%
1	1	0.218	78%

6. Implementation of the variable cross section concept.

The concept of variable cross-section spar as depicted in Figure 9 was implemented using toggle links to lock and unlock the outer spars thereby engage and disengage the outer webs. Figure 10 shows a physical embodiment of a collapsible web. Instead of using two pairs of toggle links to engage and disengage the web, a single pair was employed as shown in Figure 11(b). The variable stiffness spar was thus constructed and tested at the University of Michigan. The results indicated a 16% reduction in the torsional stiffness when the outer webs are disengaged. This is due to the fact that the cross members, i.e., the ribs contributed significantly to the overall stiffness of the spar thereby lessening the effect of unlocked spars. It was therefore decided to replace the channel sections of the ribs with upper and lower plates thereby eliminated the unwanted web section in all ribs. A physical prototype was then constructed accordingly.

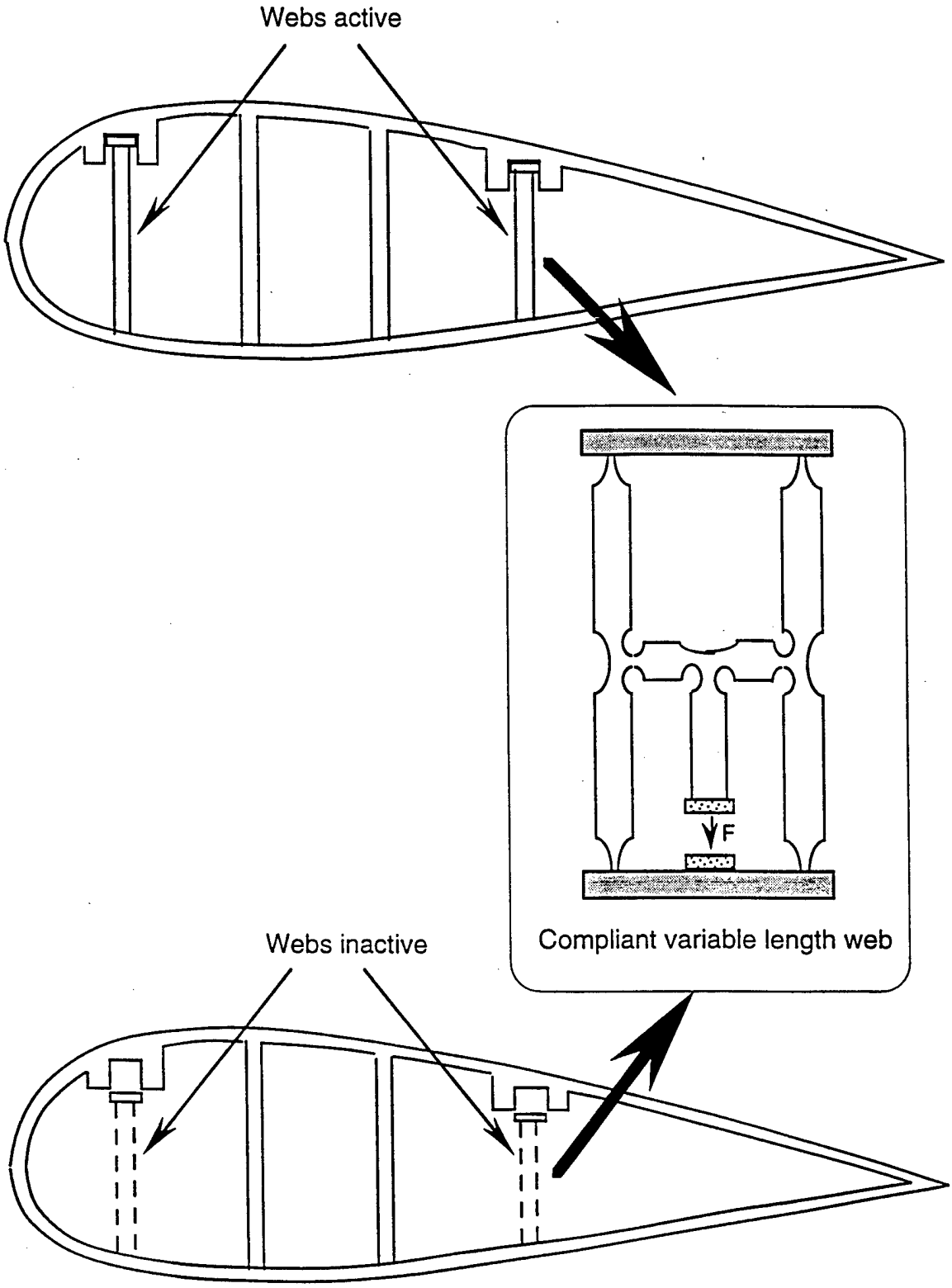

Figure 9: Practical implementation of the variable cross section collapsible-cell design concept

7. Conclusions and Recommendations

In July 1996, the PI demonstrated the physical prototype to researchers at the WPAFB and discussed the test results and theoretical predications. Figures 12-14 are photographs of the variable stiffness spar constructed at the University of Michigan. Based on these discussions, design modifications were performed and the physical prototype has been reconfigured to reflect the design changes. More specifically, the ribs of the variable stiffness spar (Designed, constructed and demonstrated by the PI to WPAFB) have been redesigned to fit the specifications of the theoretical model. The prototype has been rebuilt with new "ribs" and tested. Results showed a reduction of 30% in the torsional stiffness of the wing structure when switched to Compliant mode. Earlier prototype (Figure 12-14) showed a 16% reduction.

While this is certainly an improvement in the design it still falls short of the theoretical prediction of as much as 60% change in stiffness. One of the main reasons for the discrepancies in theory and practice is that there is a slippage between the flange and web in the channel sections since the flange and the web are two separate pieces of material. Therefore, in the stiff state, that is when the spars are "locked", the structure is less stiff in shear than the theoretical predictions due to slippage. This can be readily seen in our experimental verification of this fact, hysteresis effect, shown in Figures 15(a) and (b). Figure 16 shows the angle of twist versus the torque when the spars are unlocked. These results are also tabulated in Figure 17. The recommendation therefore is to provide interlocking teeth between the web and the flange, as shown in Figure 18, so that the channel section resists shear forces, without slippage, and remains stiff in the locked state. When this modification is implemented, it is our belief that further improvements in the ratio of torsional stiffness from stiff to complaint state can be realized.

Figure 10: Physical embodiment of a collapsible web idea.

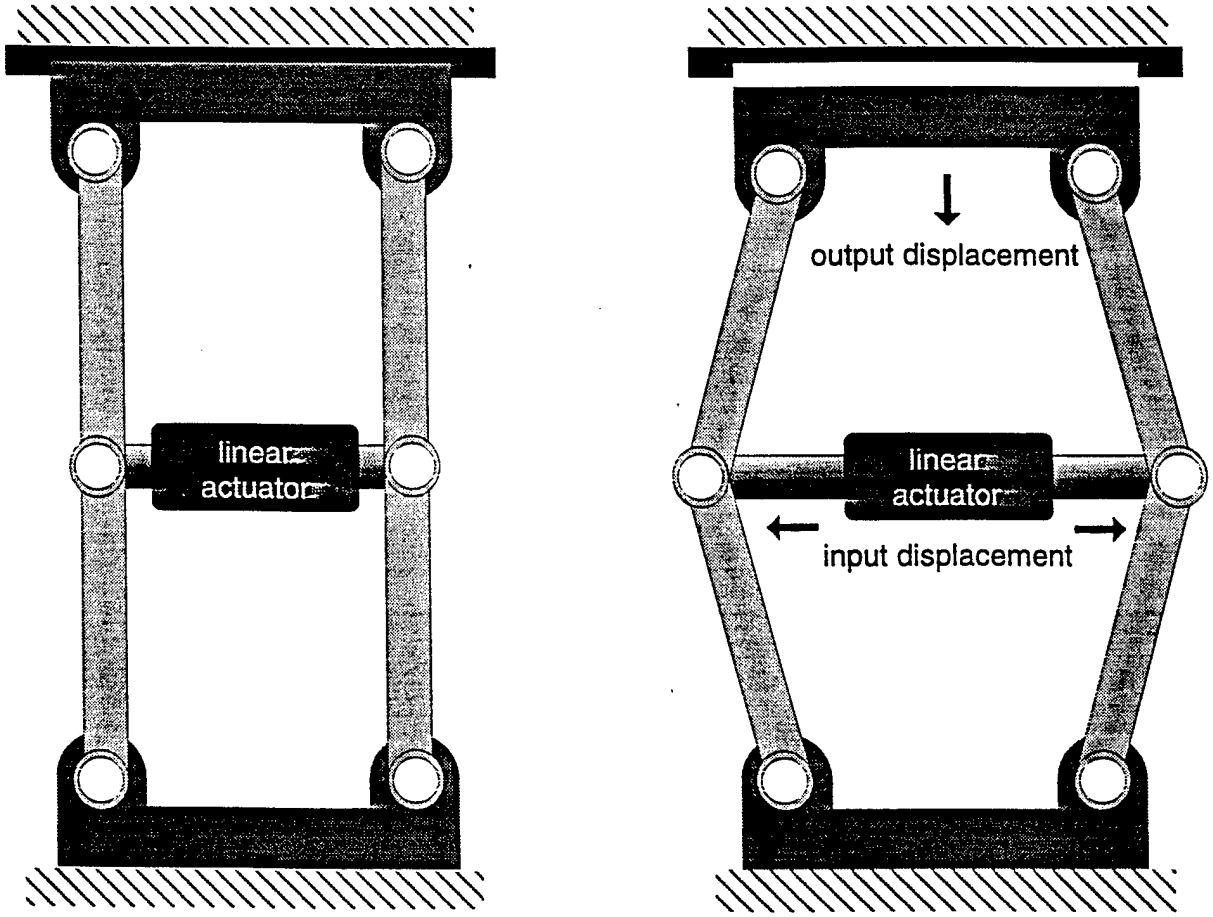

Web shown in elongated position

Web shown in collapsed position

Advantages:

- high mechanical advantage
- low frictional losses
- easily identifiable kinematic properties

Figure 11(a). Sketch of Wright Lab Wing box test bed

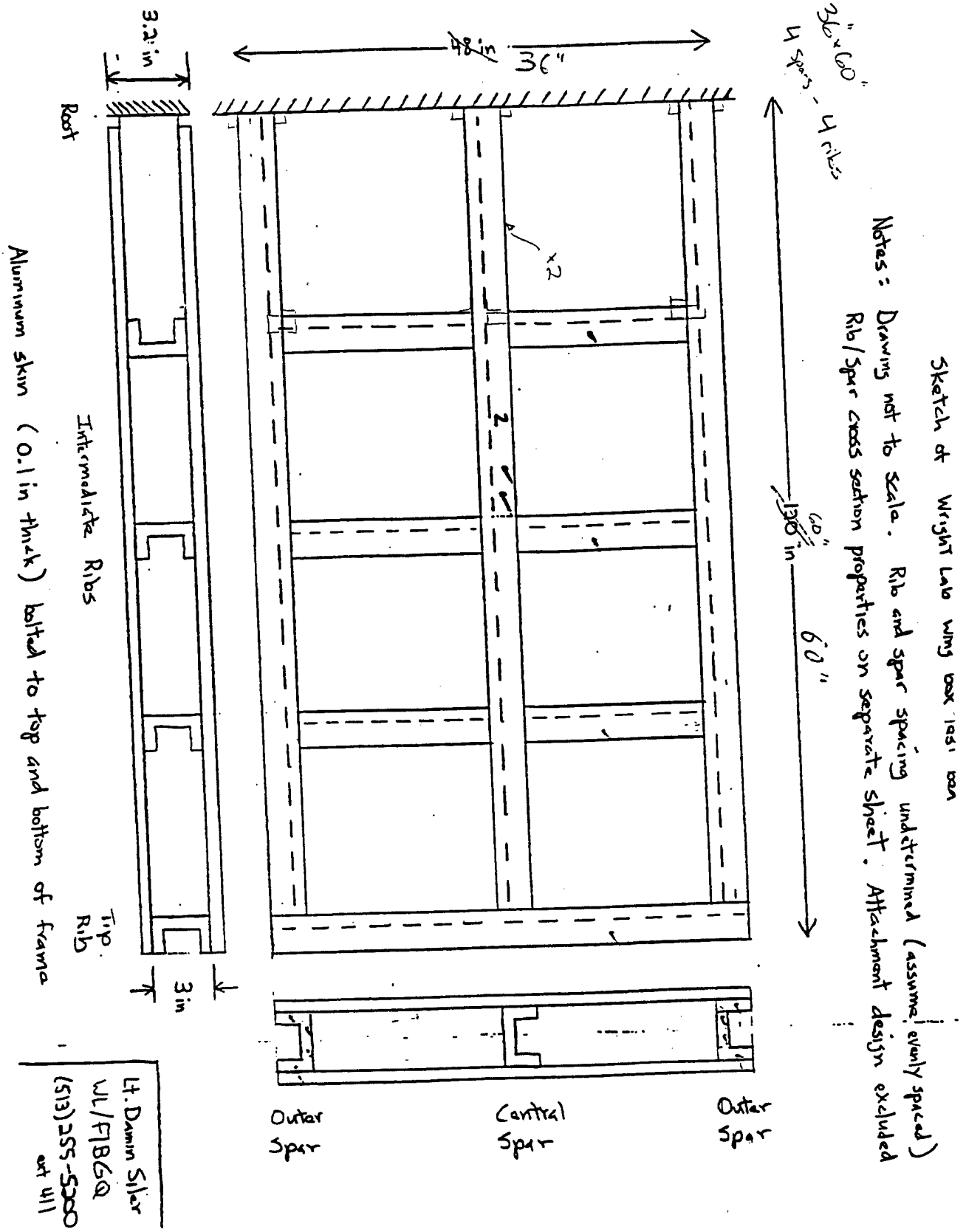

Figure 11(b): Cross-section of a variable stiffness spar based on the dimensions specified in Figure 11(a). Note that each of the collapsible spars are implemented with one-pair of links in toggle lock/unlock configuration as opposed to two-pairs of links depicted in Figure 10.

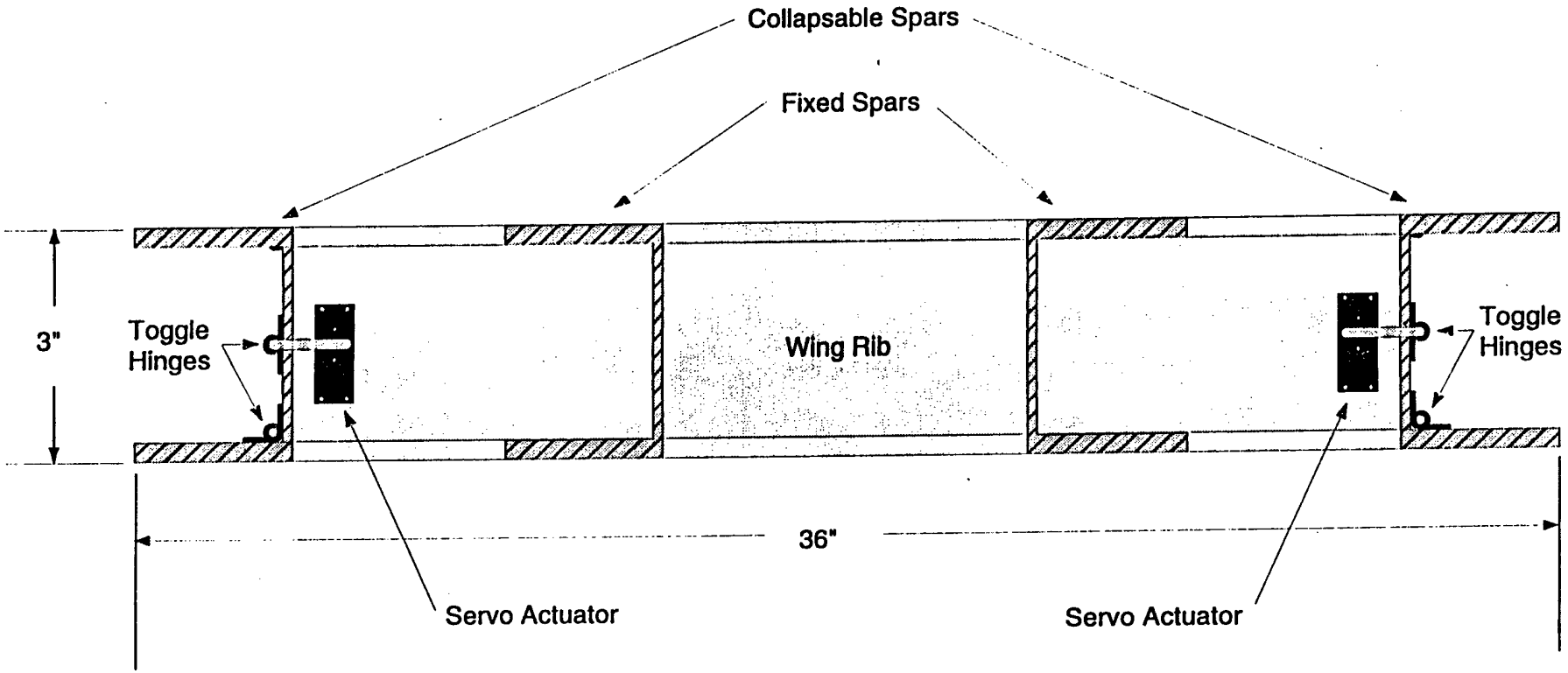

Wing Length: 60" (4 Ribs)

Figure 12 : Variable Stiffness Spar constructed at the University of Michigan using the variable cross-section concept.

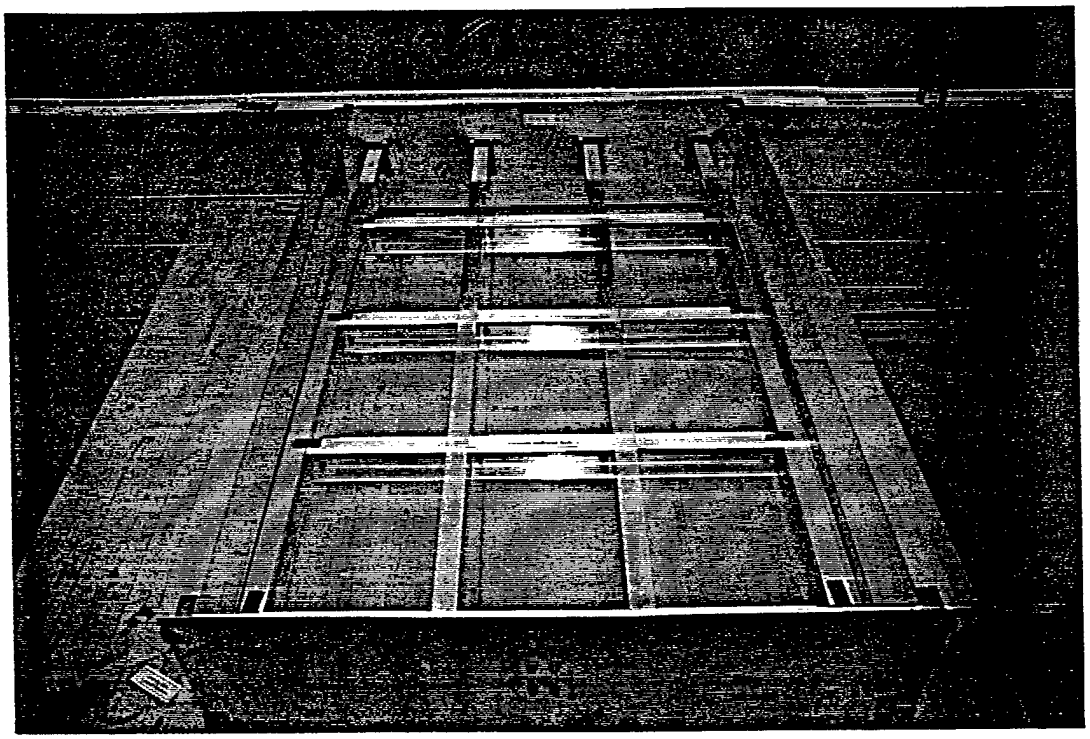

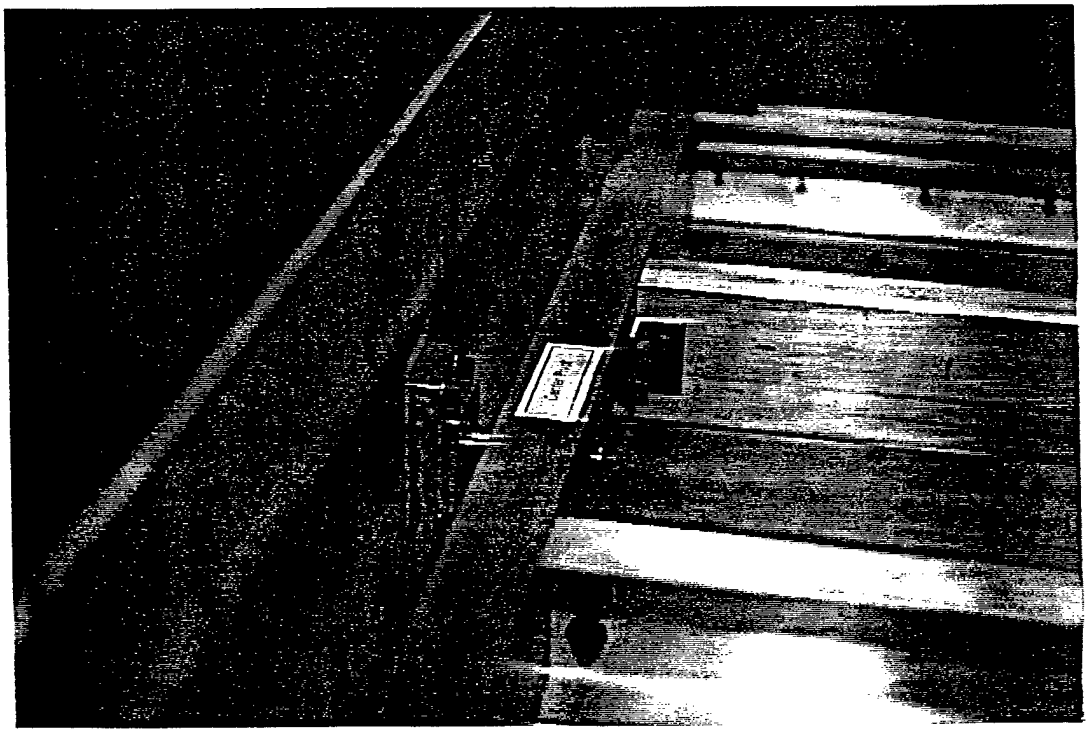

Figure 13 : Variable Stiffness Spar constructed at the University of Michigan - Spar shown in locked and unlocked positions.

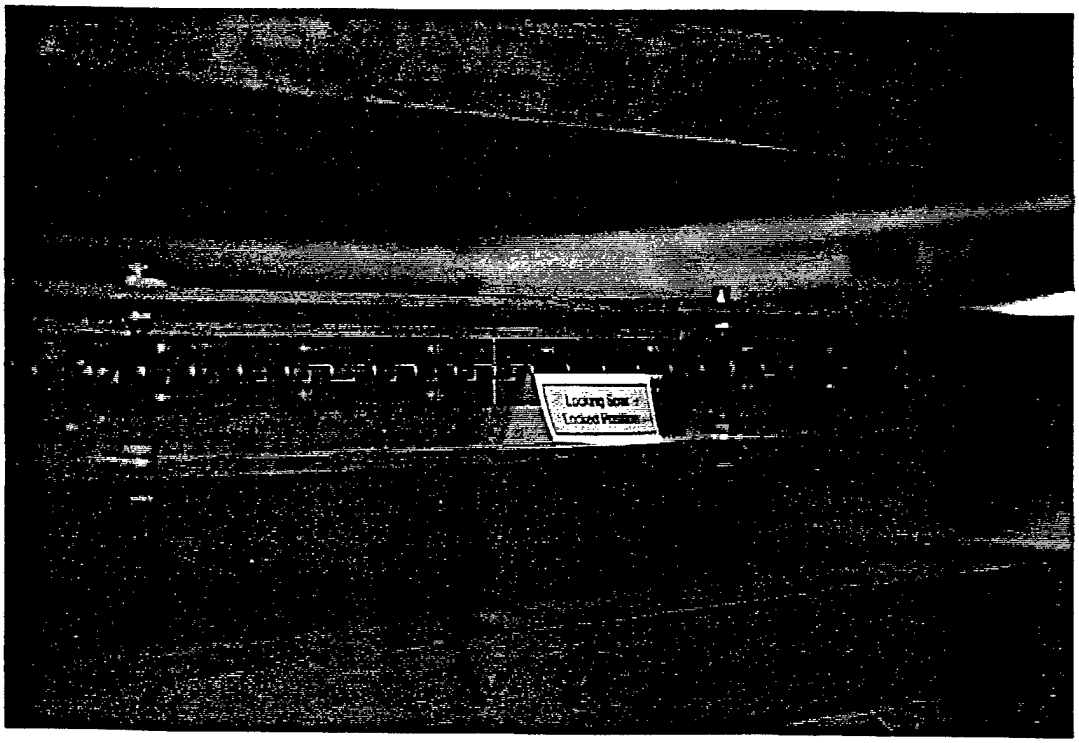

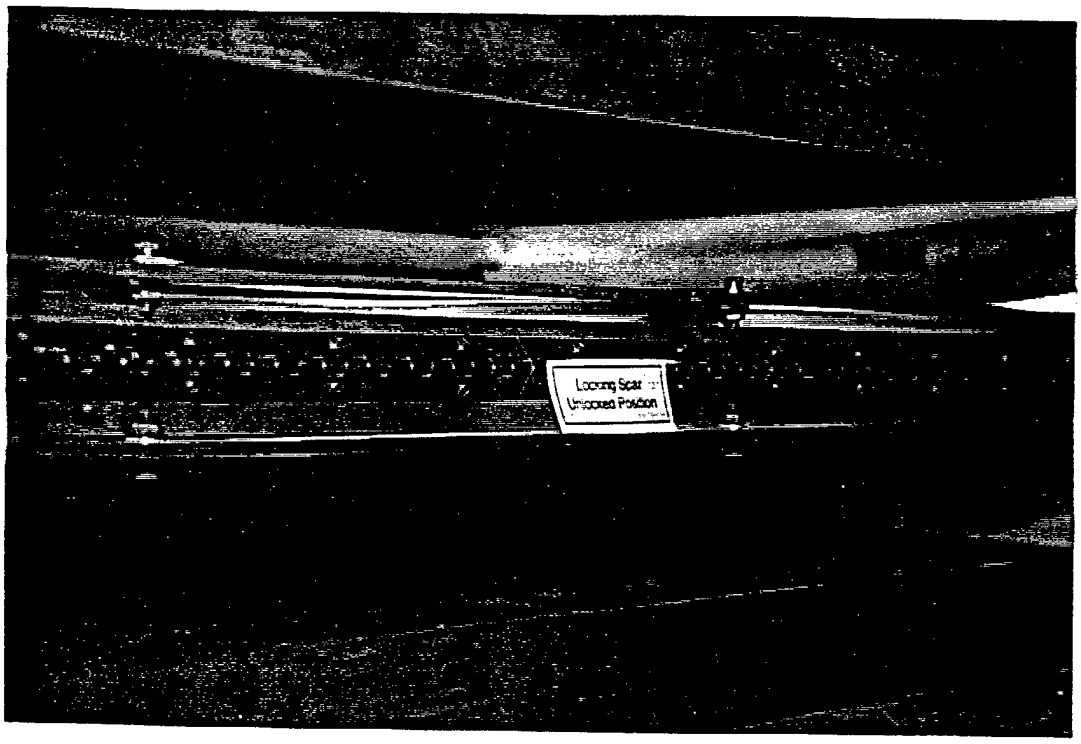

Figure 14 : Variable Stiffness Spar constructed at the University of Michigan. test apparatus.

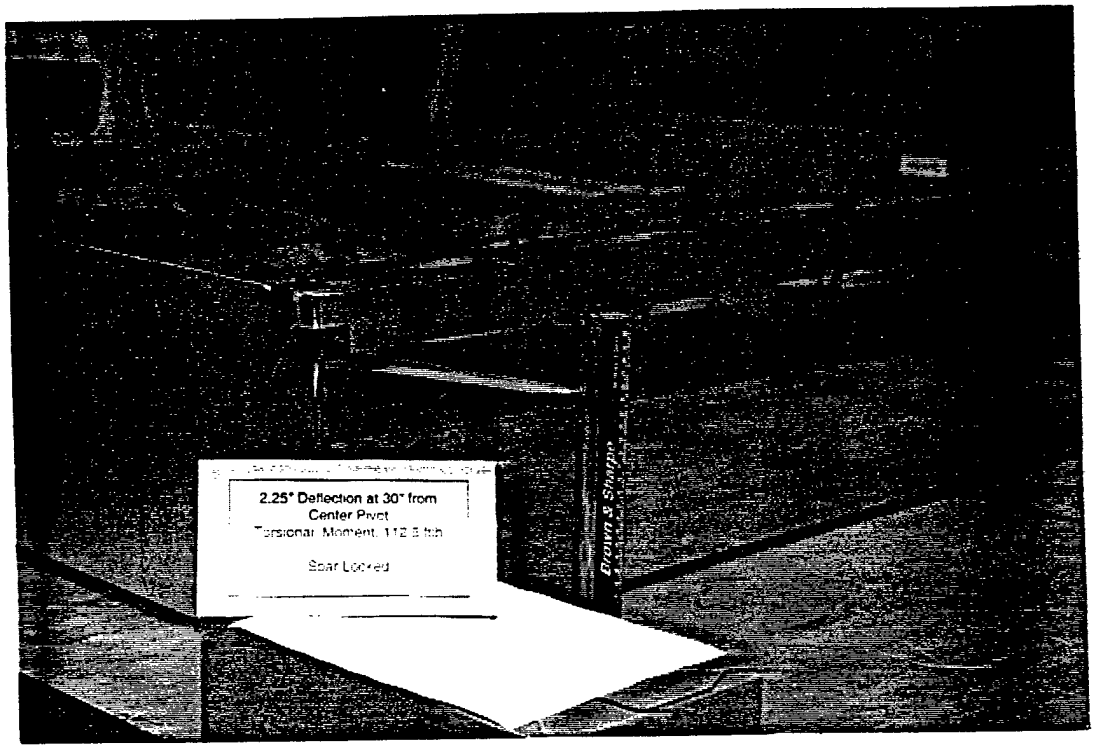

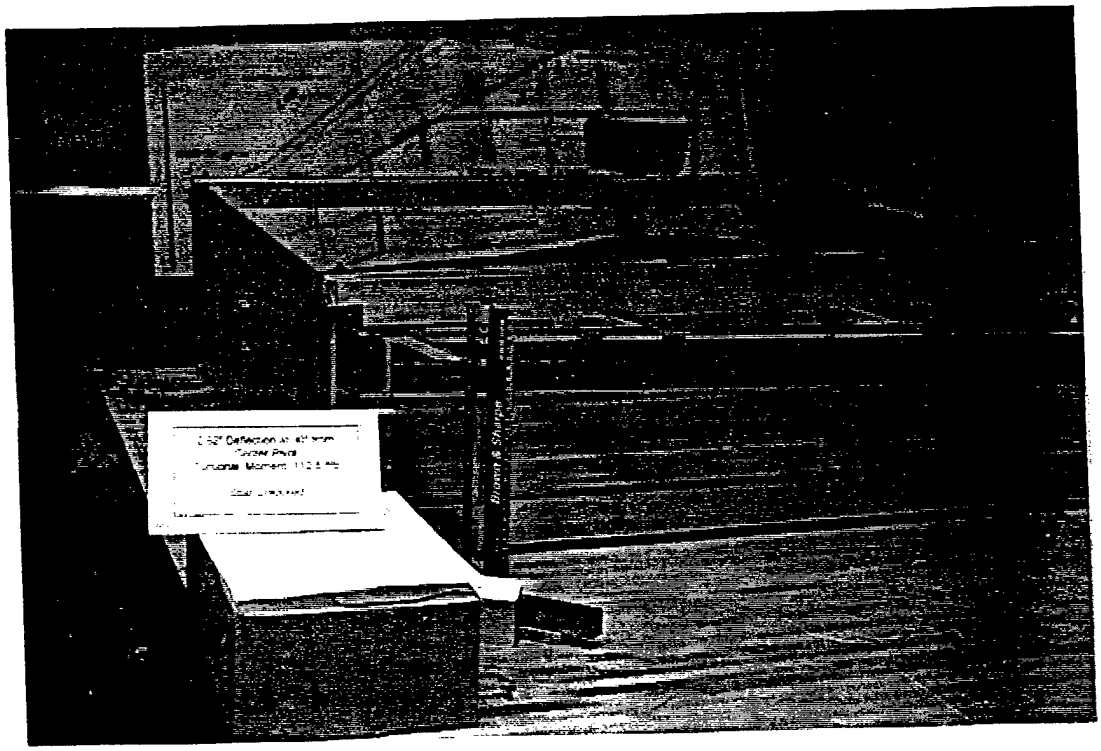

Figure 15: Applied torque versus the angle of twist of the variable stiffness spar when spars are locked. The hysteresis effect suggests slippage between the wen and the flange. (a) Left end spar. (b) Right end spar

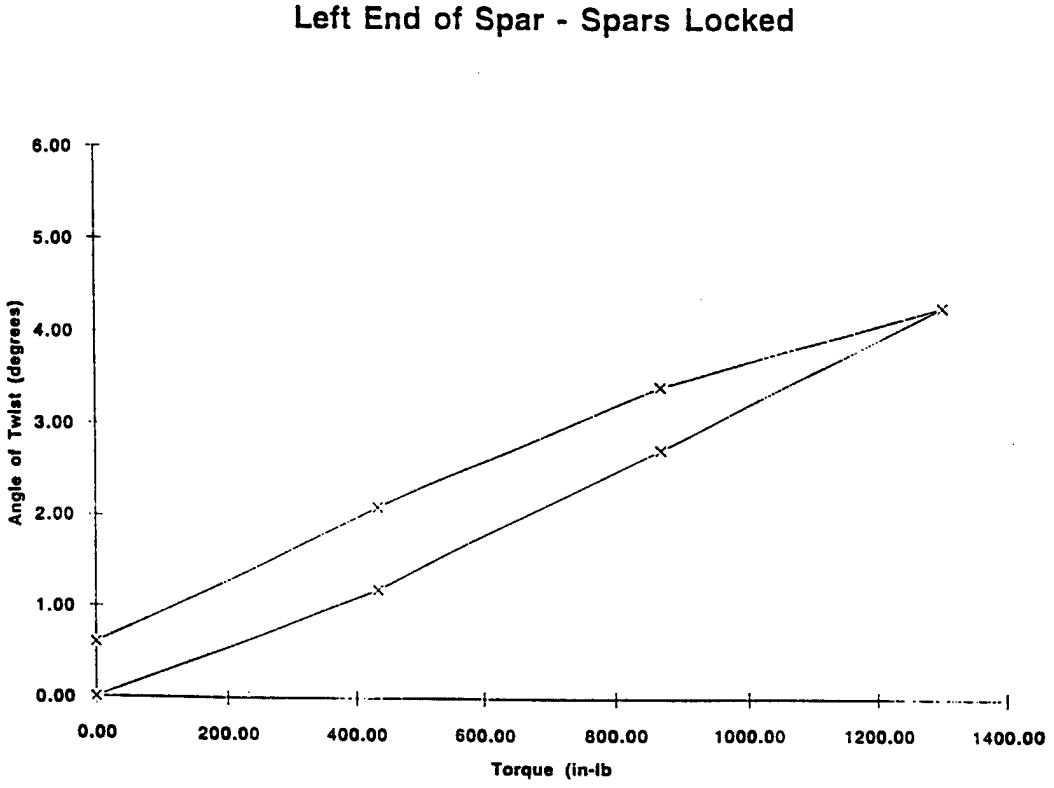

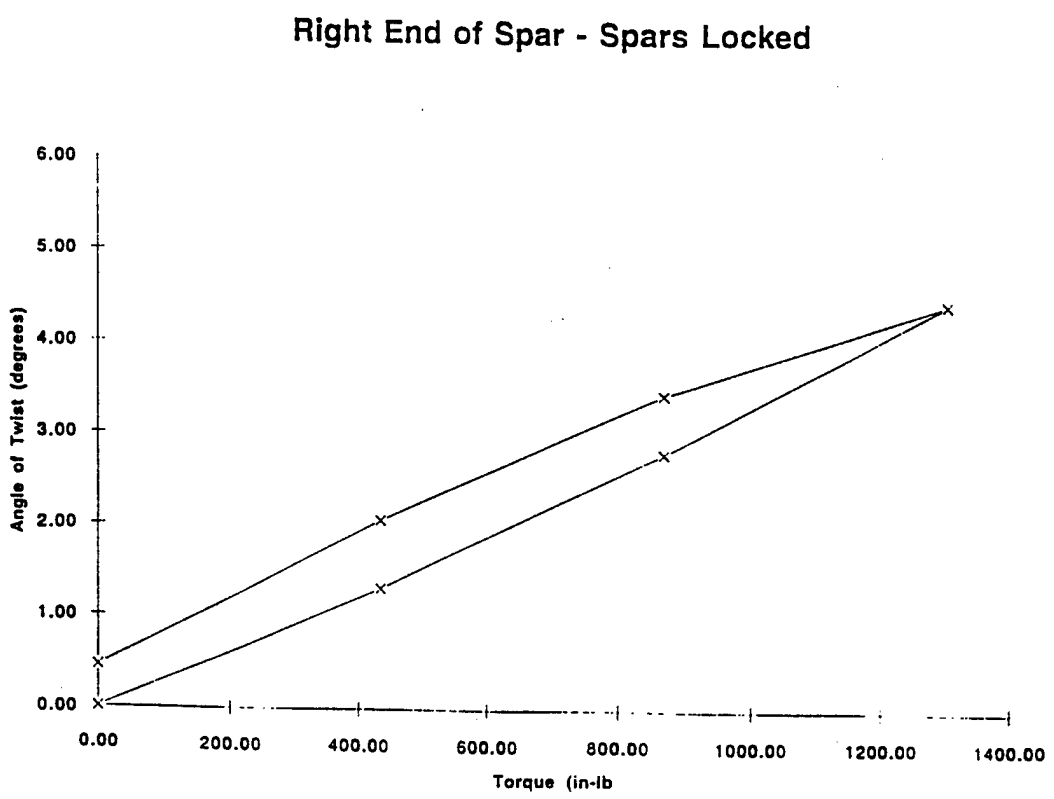

Figure 16: Applied torque versus the angle of twist of the variable stiffness spar when spars are unlocked. (a) Left end spar. (b) Right end spar

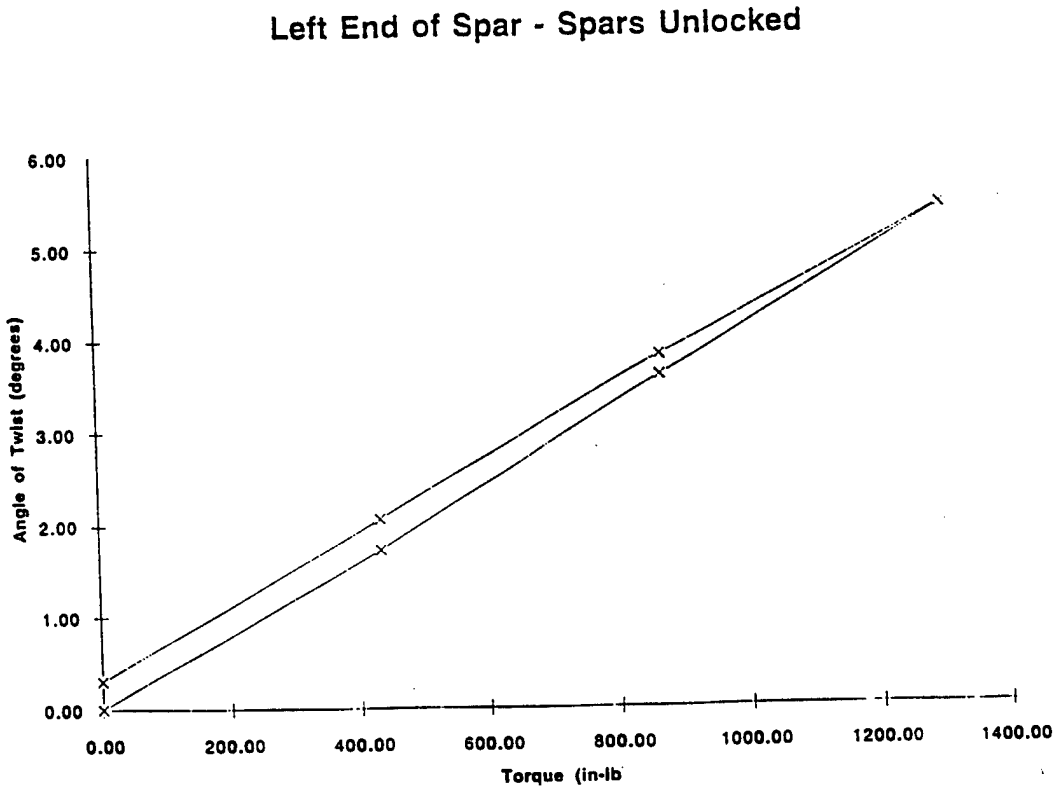

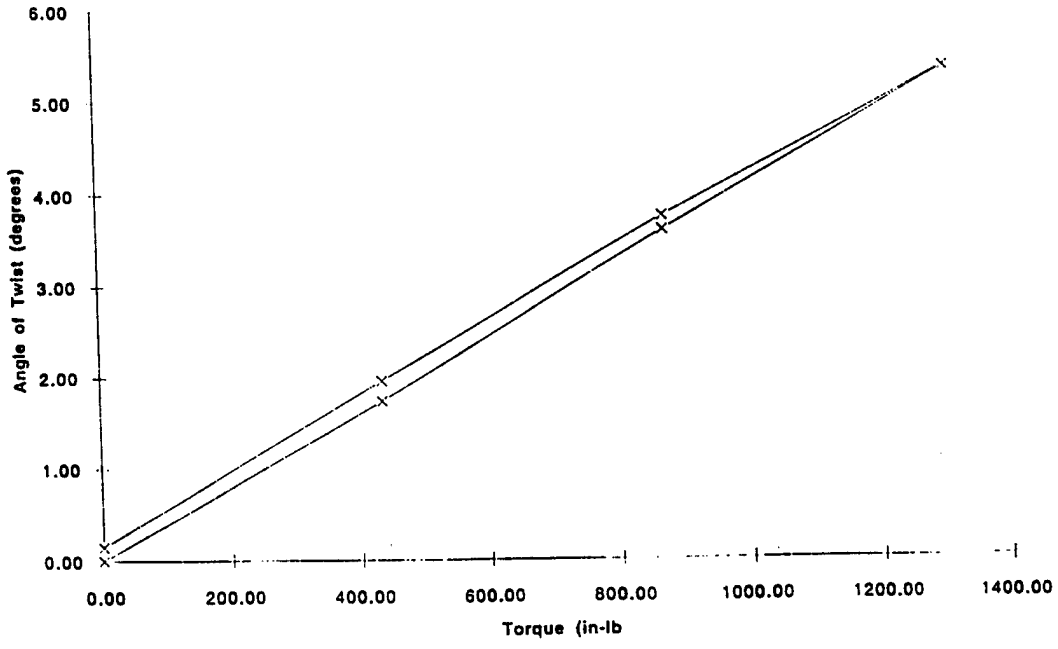

Figure 17: Various measurements made on the modified variable stiffness spar. Deflections are measured at 30 inches from the center pivot. The results showed a 30% reduction in torsional stiffness of the spar when the end spars are unlocked.

Right - Locked					
Deflection (cm)	Weight (lb)	deflection (in)	torque (in-lb)	theta (deg.)	% Δ stiffness
18.50	0.00	0.00	0.00	0.00	
16.75	25.00	0.69	434.38	1.32	23.92
14.75	50.00	1.48	868.75	2.82	21.90
12.57	75.00	2.33	1303.13	4.47	16.52
12.57	75	2.33	1303.13	4.47	
13.9	50	1.81	868.75	3.46	
15.75	25	1.08	434.38	2.07	
17.9	0	0.24	0.00	0.45	
Right - Unlocked					
Deflection (cm)	Weight (lb)	deflection (in)	torque (in-lb)	theta (deg.)	
18.60	0.00	0.00	0.00	0.00	
16.30	25.00	0.91	434.38	1.73	
13.80	50.00	1.89	868.75	3.61	
11.50	75.00	2.80	1303.13	5.35	
11.5	75	2.80	1303.13	5.35	
13.6	50	1.97	868.75	3.76	
16	25	1.02	434.38	1.96	
18.4	0	0.08	0.00	0.15	
Left - Locked					
Deflection (cm)	Weight (lb)	deflection (in)	torque (in-lb)	theta (deg.)	% Δ stiffness
9.40	0.00	0.00	0.00	0.00	
11.00	25.00	0.63	434.38	1.20	30.44
13.05	50.00	1.44	868.75	2.75	23.98
15.10	75.00	2.24	1303.13	4.29	20.88
15.1	75	2.24	1303.13	4.29	
13.95	50	1.79	868.75	3.42	
12.2	25	1.10	434.38	2.11	
10.2	0	0.31	0.00	0.60	
Left - Unlocked					
Deflection (cm)	Weight (lb)	deflection (in)	torque (in-lb)	theta (deg.)	
9.60	0.00	0.00	0.00	0.00	
11.90	25.00	0.91	434.38	1.73	
14.40	50.00	1.89	868.75	3.61	
16.80	75.00	2.83	1303.13	5.42	
16.8	75	2.83	1303.13	5.42	
14.7	50	2.01	868.75	3.84	
12.35	25	1.08	434.38	2.07	
10	0	0.16	0.00	0.30	

Figure 18: Recommendation to use interlocking teeth between the flange and the web in the end spars to prevent slippage in the locked state.

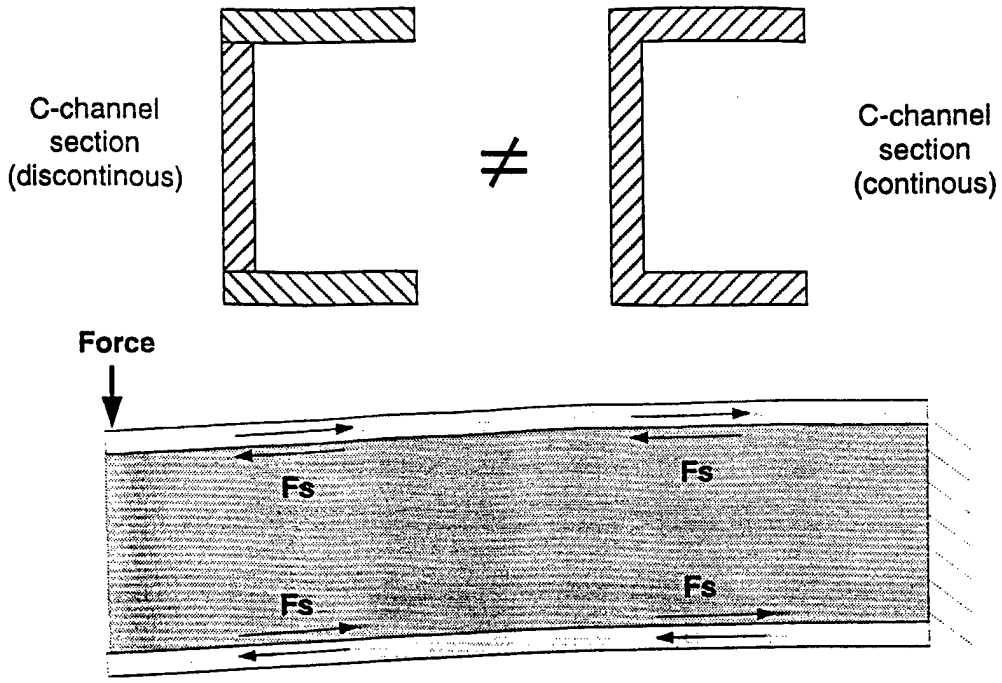

In a standard beam, a percentage of bending loads are transfered through beam sections through shear forces, Fs. Because the beams used in the Variable Stiffness Spar are not continuous, no shear forces are transmitted and the resulting structure is not as stiff as theoretically predicted.

The solution to this problem is to modify the beam sections so that they may transfer these shear loads to increase the stiffness of the entire structure.

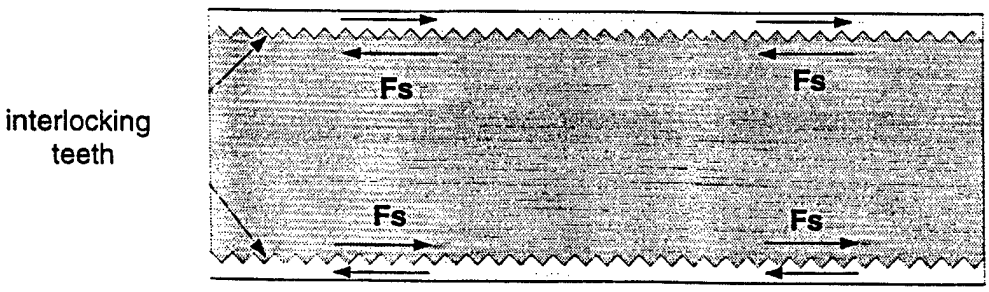

one possible modification to improve shear force transmission through beam sections